WPMST1-PR(17) 17944

D Kim et al.

Sawtooth control experiment on ASDEX Upgrade

Preprint of Paper to be submitted for publication in Nuclear Fusion

This work has been carried out within the framework of the EUROfusion Consortium and has received funding from the Euratom research and training programme 2014-2018 under grant agreement No 633053. The views and opinions expressed herein do not necessarily reflect those of the European Commission.

Sawtooth control experiments on ASDEX Upgrade

D. Kim *[1,2], I. T. Chapman[3], O. Sauter[1], T. P. Goodman[1], J. H. Jeong[4], the ASDEX Upgrade Team[5], and the EUROfusion MST1 Team[†]

[1]École Polytechnique Fédérale de Lausanne (EPFL), Swiss Plasma Center (SPC), CH-1015 Lausanne, Switzerland
[2]ITER Organization, Route de Vinon-sur-Verdon, CS 90 046, 13067 St.-Paul-lez-Durance Cedex, France
[3]CCFE, Culham Science Centre, Abingdon, UK
[4]NFRI, Daejeon, South Korea
[5]Max-Planck-Institut für Plasmaphysik, Garching, Germany
[†]See the author list of Overview of progress in European Medium Sized Tokamaks towards an integrated plasma-edge/wall solution by H. Meyer et al., to be published in Nuclear Fusion Special issue: Overview and Summary Reports from the 26th Fusion Energy Conference (Kyoto, Japan, 17-22 October 2016)

August 4, 2017

E-mail: dkim@pppl.gov

Abstract

The capability of active sawtooth control using electron cyclotron heating and current drive (ECH/CD) has been investigated in the ASDEX Upgrade (AUG) 2014 campaign. Based on the successful sawtooth control experiments performed on TCV (Tokamak à Configuration Variable) and KSTAR (Korea Superconducting Tokamak Advanced Research), we have applied the sawtooth locking method to AUG plasmas with various modulation periods and duty cycles. Sawteeth did not lock to the EC modulation in AUG experiments, though in some discharges they became somewhat more regular. The sawtooth behaviour of AUG plasmas was more complicated compared to TCV and KSTAR due to the fast particle effect on the evolution of sawtooth from both neutral beam injection and ion cyclotron heating. Furthermore, various experiments conditions were examined in one discharge thus more investigation with simpler conditions is required in order for the feasibility of sawtooth locking to be examined. The experimental results were compared to those from TCV, KSTAR and ITER predictive sawtooth simulation result. The normalised time difference between the sawtooth crash and the moment of the EC power turning off shows a good agreement among those experimental and simulation results. More experiments at AUG should follow to understand better the behaviour of sawteeth and to determine the sawtooth locking range.

1 Introduction

The sawtooth instability in tokamak plasmas is characterised, on temperature and X-ray measurement time traces, by periodic fast relaxations followed by a slower recovery of the signal amplitude in the central region where the safety factor q is lower than unity [1]. The fast relaxation (crash) following a long delay between crashes (sawtooth period) can create a seed island, triggering neoclassical tearing modes (NTMs) that limit the safe operating regime of the tokamak [2, 3]. A second consequence is a lowering of the β limit for NTM onset by more than a factor of two, resulting in NTMs triggerred at low β_N [4]. Therefore, it would be helpful to control the sawtooth period and to know when the next sawtooth crash is likely to occur in order to avoid NTM triggering. This is particularly important for ITER, since relatively long sawtooth periods, produced by energetic α-particle stabilisation, are predicted in ITER [1]. Foreknowledge of the crash time would allow us to add EC power on the $q = 3/2$ and/or

*present address: Princeton Plasma Physics Laboratory, Princeton, USA

2/1 surface before the islands are triggered, potentially preempting the formation of large NTMs, as was demonstrated on TCV [5, 2].

The simplest strategy for preventing NTMs, triggered by sawtooth crashes, is to destabilise the sawteeth (i.e. to shorten the period as much as possible) by driving continuous wave ECCD in the direction of plasma current near the centre. In this case, the sawtooth period may be short enough to avoid NTM triggering [6, 7, 8, 2]. However, if the resultant sawtooth period is still too long (i.e. the shortest sawtooth crashes do trigger NTMs), then sawtooth period stabilisation together with NTM preemption will be required.

Recent TCV experiments have shown that sawtooth pacing [9] and locking [10, 11] are two efficient ways to control the sawtooth period using EC power pulses. For pacing, EC power is turned on for a given time period by a real-time control system once a crash is detected; whereas the on-off timing (both period and duty cycle) is determined a priori for locking, so that no real-time control is necessary. Using either method, sawtooth period can be regulated and the moment of the NTM onset after a sawtooth crash can be predicted. Similar to TCV experiments, recent KSTAR experiments have also shown that sawtooth periods are regulated using the sawtooth locking method [12].

Despite the successful demonstration of TCV and KSTAR sawtooth control experiments, more experiments with various plasma conditions from different tokamaks are still required. With sufficient experimental results, it should be possible to set a scaling law for prediction of sawtooth crash controlled by EC modulation and the subsequent triggering of NTMs; the goal being to apply the scaling to ITER plasma for predicting the sawtooth crashes so that NTMs can be preempted using EC injection prior to the creation of NTM seed island.

In this work, we show the results of sawtooth control experiments in ASDEX upgrade (AUG), where the sawtooth locking method has been applied. Since the specific real-time control algorithms required for sawtooth pacing were not yet in operation at the time of these discharges, only sawtooth locking was investigated experimentally.

In the remainder of this paper; the prediction of locking range and the experiment set up and EC beam sweeping experiment will be presented in Sec. 2. In Sec. 3, the experimental results will be discussed as well as the comparison to similar experimental and simulation results from other tokamaks. Finally, conclusions are provided in Sec. 4.

2 Preparation of sawtooth locking experiment

2.1 Prediction of locking range

Prior to the experiment, we have done simulations using the transport code ASTRA [13] to predict a possible locking range for the reference discharge AUG #30233 (experimental data is taken from 4.0s). In Fig. 1, the T_e, T_i, n_e, n_i, power and current densities and q profiles evaluated by the simulation (dashed line) are presented with the reference data (solid). For the T_e and n_e evaluation, the transport model described in Ref. [14] using H factor of 0.85 and fixed R/L_{n_e} of 1.5 has been taken. T_i is evaluated using formulae from neoclassical theory [15] and n_i is assumed to be proportional to n_e. All the profiles are modified by the sawtooth crash. For sawtooth modelling, full reconnection [16] and sawtooth crash criteria from Refs. [1, 17] are used. Auxiliary heating powers of NBI (7MW) and central ECH (0.7MW) are applied. Note that all the simulated profiles shown in Fig. 1 are those of just before a sawtooth crash.

It was verified that ASTRA simulation can reproduce reference data and that therefore ASTRA simulation with the given setting can be used for the sawtooth locking simulations. At first, an EC beam sweeping simulation was performed to find the optimum position [18, 19] for sawtooth locking. In the reference experiment (#30233), a 0.7MW EC beam was deposited at the plasma centre. However, in the sawtooth locking experiment shown later, more EC power is expected. Thus in this simulation, it is assumed that another 0.7MW EC beam is added to deposit 1.4MW EC power in total. Both EC beams are swept across the minor radius from the centre to the edge. The estimated sawtooth period from the simulation is 65ms with an EC beam at the centre (0.7MW, match the experimental period) while it is 140ms without a central EC beam. From the sweeping, the maximum period of 600ms is found without central EC heating and current drive. We have chosen the EC deposition position ($\rho_\psi \sim 0.41$) where the corresponding sawtooth period is about 480ms and several tests for sawtooth locking were performed using this fixed beam location. Note that in this simulation, it is not the goal to have the maximum sawtooth period so that we chose a deposition position near the $q = 1$ surface (slightly outside in this case) to have a sufficient stabilising effect (140 to 480ms) for sawtooth locking tests.

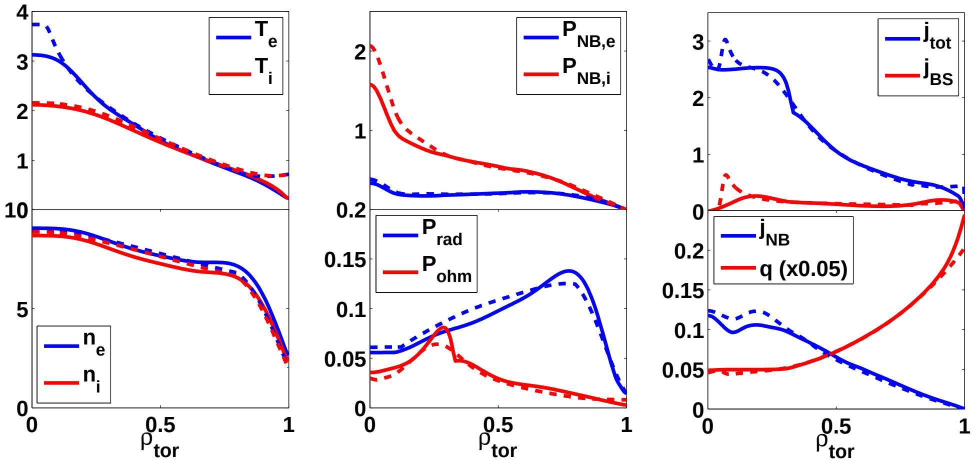

Figure 1: Profiles calculated from ASTRA (dashed) and reference data (solid) from AUG #30233 4.0s. Left: Kinetic profiles (T_e, T_i, n_e, n_i) evaluated using the transport model (T_e, n_e) from Ref. [14] and neoclassical theory (T_i) show good agreement with the reference ones. NBI power contributions to electron and ion, radiated and ohmic powers in the middle panels and current density (j_{tot}, j_{BS}, j_{NB}) and q profiles in the right panels from ASTRA are also well matched to reference data.

Three modulation periods of 200, 250 and 450ms are taken for the locking simulation. For the 200ms case, sawteeth lock to the modulation period when the duty cycles are between 20 and 80%, while it is between 40 and 80% for the 250ms case. For long modulation period (450ms), sawteeth lock to EC modulation only for very large duty cycles (80 and 90%). Since the sawtooth periods from the simulation may be different from those of the actual experiment, the modulation periods are normalised as $\tau_{normalised} = (\tau_{set} - \tau_{ref})\,/\,(\tau_{CW} - \tau_{ref})$, where τ_{set} is the chosen modulation period and τ_{ref} and τ_{CW} are the sawtooth periods without (i.e. the "reference" case, 140ms) and with continuous (CW, 480ms) EC beam, respectively. The simulated periods correspond to 0.177 (200ms), 0.324 (250ms) and 0.912 (450ms) in the normalised values. The estimated locking cases (green square) are shown in Fig. 2 with simulation and experimental results that will be discussed in Sec. 3. From these simulation results, one can gain intuition for choosing modulation periods and duty cycles for the locking experiments, even though the maximum and reference periods may differ from the experimental result and the simulation results are not enough to complete the locking range. For instance, in the experiment, one can expect $\tau_{normalised} \sim 0.5$ as an option for obtaining both locking and unlocking cases or duty cycle of 80∼90% to explore the boundary of the locking range. It should be noted that this simulation result was used to have an idea for the experiment, not to directly be applied for the experiment, which may have different plasma states. Thus the EC beam deposition position, modulation periods and duty cycles applied in this simulation are not necessarily the same in the experiments and these values will be confirmed by experiments.

2.2 Experimental set up

For the series of discharges comprising the sawtooth locking experiment, a fixed value of $I_p = 1.0$MA is taken and n_e is around $7.0\times10^{19}\text{m}^{-3}$. For the auxiliary heating, 7.0MW NBI, 1.7MW IC and 1.8MW EC powers are delivered to the plasma. The IC power is deposited at the plasma centre and three EC beams, each with a power of 0.6MW, are used. One beam continuously deposits power on axis to expel the impurities in the central region (tungsten accumulation avoidance) and the other two modulating beams aim near the $q = 1$ surface for sawtooth locking. Note that in the predictive simulation, IC power was not applied, two EC beams were located around the $q = 1$ surface and no central EC power was deposited. Therefore, in the experiment, a shorter sawtooth period is anticipated with respect to the simulation, since central heating decreases the sawtooth period. In Fig. 3 the scenario time traces and ECH and ECCD profiles from a beam tracing code TORBEAM [20] are shown. The flattop of I_p and n_e occurs from 1.0 to 8.0s. During the flattop phase, NBI power is injected from three ports, in steps, and afterwards IC and EC power injections follow. To investigate sawtooth locking, EC power is modulated

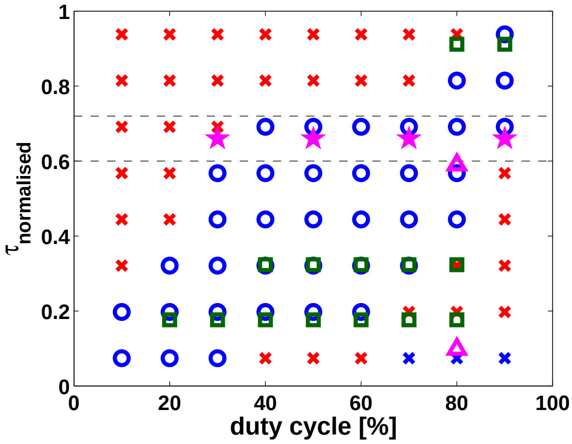

Figure 2: Predictive simulation results based on AUG #30233 (green square) are depicted on the normalised locking range with simulation results of the discharge #30543 (blue-locking; red-no locking) and experiment cases (will be discussed in Sec. 3). Both results from #30550 (star) and #30552 (triangle) cases are not precisely same but similar to the simulation result.

with pre-set modulation period and duty cycle. Several combinations of period and/or duty-cycle have been used in each discharge. With this set up, sawtooth locking experiments are conducted.

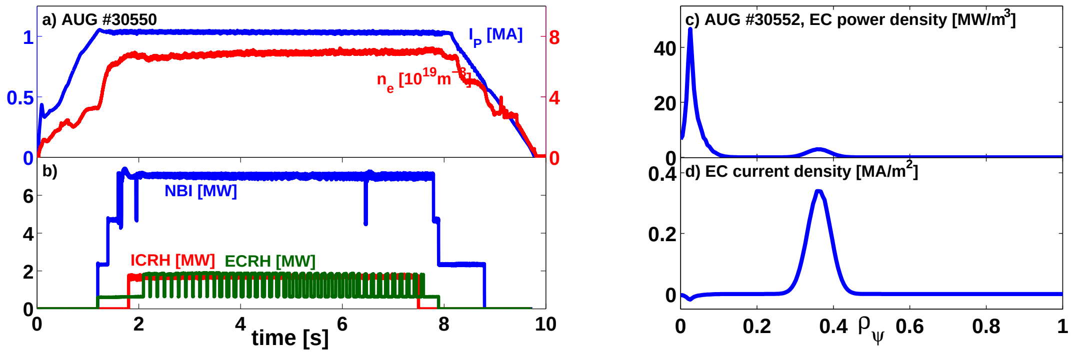

Figure 3: (a) I_p and n_e are kept constant to 1.0MA and $7.0{\times}10^{19}\mathrm{m}^{-3}$ during flattop phase. (b) NBI, IC and EC power heat the plasma with 7.0, 1.7 and 1.8MW, respectively. NBI, IC and one central EC powers are continuously injected while two EC beams are modulated for sawtooth period control. (c, d) One EC beam is located in the plasma axis for heating and two other beams are deposited on nearby $q = 1$ surface for current drive.

2.3 EC beam scan across plasma radius

In order for the EC beam deposition position to be determined, a poloidal scan of EC power has been performed in the AUG discharge #30543. The central EC beam is turned on at 1.1s and the two sweeping beams are switched on at 2.1s. During the first 1.0s of the current flattop, NBI power is increased in steps and IC deposition begins. As a result, the reference sawtooth period - τ_{ref} without sawtooth-control EC beams - cannot be determined from this phase of the discharge; instead, it is estimated from the phase when EC beams are far outside the $q = 1$ surface since it has been previously shown that the sawtooth period returns to the reference period under these conditions during unmodulated sweeps [21, 22]. Two beams sweep from $\rho_\psi \approx 0.2$ to 0.6 between 2.1 and 4.6s. The central temperature measured by ECE and the applied EC power are plotted in Fig. 4a and the deposition position of EC beams and the resultant sawtooth period τ_{ST} are shown in figures 4b and 4c, respectively. When EC power is deposited in the central region, τ_{ST} becomes short, around 10ms and irregular. τ_{ST} increases as EC beams approach the

$q = 1$ surface and around 3.7s, the maximum τ_{ST} of 165ms is obtained when EC beams are located at $\rho_\psi \approx 0.45$ (dashed line area). Once the EC beams cross the $q = 1$ surface, τ_{ST} rapidly decreases and stays around $60 \sim 70$ms until the end of the sweeping. This period can be referred to as τ_{ref} since EC beams deposited far outside the $q = 1$ surface have a small effect on τ_{ST}. As observed on TCV, the τ_{ST} associated with a crash time is actually an average value obtained while the EC beams scan over the positions immediately preceding the crash. The fixed deposition position of $\rho_\psi = 0.42$ was chosen, assuming it would correspond to a maximum $\tau_{ST} \approx 150$ms, for the locking experiments described here. Note that the EC sweeping across the plasma minor radius is relatively fast compared to the energy confinement time $\tau_E \sim 70$ms (without control EC beams). A slower reduced range sweeping should be conducted for a more precise determination of the optimal position. However experimental constraints led to very few discharges dedicated to locking experiments. As seen in Fig. 4, the sawtooth period decreases rapidly once the EC beams pass the maximum position, this is why it is safer to choose a timing a bit earlier when sweeping from inside to outside the $q = 1$ radius.

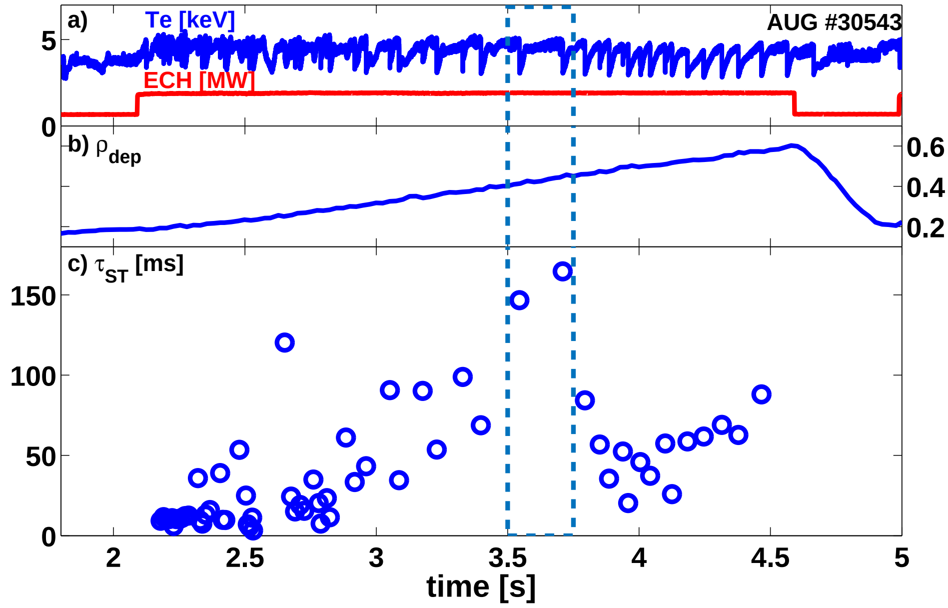

Figure 4: From 2.1s two control EC power sources are switched on and start sweeping from 0.2 to 0.6 in ρ_ψ. τ_{ST} increases as EC beams approach close to the $q = 1$ surface and has the maximum value of 165ms at $\rho_\psi = 0.45$. For the further sawtooth locking experiment, the fixed EC deposition position is set to $\rho_\psi = 0.42$ which is expected to bring τ_{ST} to 150ms.

3 Sawtooth locking experiments with various modulation periods and duty cycles

Based on the results from the sweeping experiment and simulation, sawtooth locking experiments by injecting modulated EC power are carried out. Prior to the discussion, it is worth to remind that from the predictive simulation using #30233 data, we chose the modulation periods between 140 (reference) and 480ms (CW EC injection of 1.4MW) without central IC heating and EC heating and current drive. For the experiments, the chosen modulation periods are based on the sweeping experiment (#30543), which has IC heating and EC heating and current drive at the centre. The different auxiliary heating scheme brings much shorter feasible modulation period, between 65 and 150ms. However, we can still apply the similar normalised modulation period and duty cycle from the simulation. For the first test, we have fixed a modulation period τ_{set} with various duty cycles in the AUG discharge #30550. With fixed deposition position at $\rho_\psi = 0.42$, a period of 150ms is anticipated. Based on the simulation results, the normalised modulation period of about 0.4 which corresponds to 100ms is used for the EC modulation period (it is expected that sawteeth lock to EC modulation from 40 or 50 to 80%).

The actual deposition pulse (EC on-time duration) is determined by the duty cycles of 90, 70, 50 and 30%. However, an incorrect EC control command caused a modulation period of 140ms (normalised period$\sim$0.88) in the actual experiment, producing non-optimum behaviour worth discussing here. Fig. 5 shows the experimental results. In the top panel the central electron temperature and injected EC power time-traces are plotted. τ_{ST} and τ_{set} are presented in the mid-panel (Fig. 5*b*) as blue circles and red line, respectively, and the bottom panel shows the duty cycle.

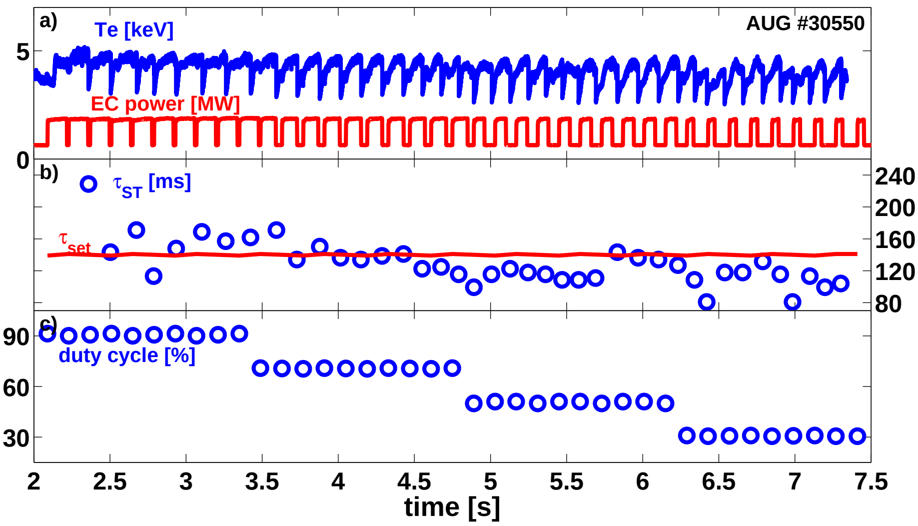

Figure 5: A sawtooth locking experiment with τ_{set} of 140ms and various duty cycles. When the EC power is switched on and starts modulation, the plasma changes considerably and needs time to settle down. In this transient phase, a long sawtooth crash occurs and then τ_{ST} becomes about 160ms in the 90% duty cycle case. With 70% duty cycle, there are a few sawteeth which have similar periods as τ_{set}. In the 50 and 30% phases, τ_{ST} varies much compared to the previous two duty cycle cases. There is no clear sawtooth locking, except a few near 6s and the average τ_{ST} in each duty cycle phases decrease with reduction of averaged power for each phase.

At 2.1s, control EC beams are switched on and bring changes in the plasma state. During a transient phase, a very long sawtooth with period of 230ms occurs and then τ_{ST} decreases. During this phase, the modulation does not have much effect; since the duty cycle is 90%, EC beams are nearly always present. After the first several sawtooth crashes, τ_{ST} becomes close to 160ms, which is longer than τ_{set} and shows the expected maximum period is about 165ms - corresponding to the maximum value found during the sweep shown in Fig. 4. Since the effect of EC injection on sawtooth period is dependent on the distance between the beam deposition position and the $q = 1$ surface, if the $q = 1$ surface location is different, the resultant sawtooth period can be different with the same beam set-up. In this discharge, the maximum sawtooth period is larger than 150ms, showing that the plasma state is different from the sweeping discharge (#30543). Note that the effective relative positions of the $q = 1$ surface cannot be obtained with a sufficient accuracy, but the effects on sawteeth are actually an accurate measure of such differences.

The duty cycle decreases to 70% at 3.5s. At the beginning of this phase, τ_{ST} is still long but after a few sawtooth crashes becomes similar to τ_{set} which may indicate that the system is close to locking. Regular sawteeth do not last long and τ_{ST} slightly decreases (after 4.5s) under the same modulation condition, indicating that locking has not occurred: for true locking the phasing of the pulses to the sawteeth should stabilise at a near constant value. For the 50% duty cycle case, τ_{ST} varies between 100 and 120ms. At the end of the phase, τ_{ST} suddenly increases and stays around 140ms. With 30% duty cycle, τ_{ST} has a wider variation, between 80 and 130ms. At first, τ_{ST} decreases from the period it had at 50% duty cycle and then, at a certain moment, a complete sawtooth cycle occurs during the EC-off duration, since that duration is longer than τ_{ref}. Note that the τ_{ST} during the off duration is 80ms, which is longer than the expected reference period. This is because the plasma is still evolving due to the change of EC power - if EC power is turned off for a long time, τ_{ST} is anticipated to decrease to around 60ms. The delay between a crash and EC turn-off time (i.e. the "phase") is not constant.

As a result, sawteeth are not regulated by the EC modulation and there are only a couple of complete sawtooth cycles that occur during EC-off duration.

In this experiment, there is no clear sign that sawteeth lock to the EC modulation. Only a few crashes have similar τ_{ST} as τ_{set} for the 50 and 70% duty cycle cases. On the other hand, the overall sawtooth behaviour depends on the averaged injected power. Since τ_{set} is fixed and the duty cycle decreases, the averaged powers for each duty cycle phase decrease. As the averaged power is reduced, the resultant τ_{ST} decreases as well. The averaged τ_{ST} are approximately 152, 137, 120, 110ms at 90, 70, 50, 30% duty cycle, respectively. Therefore, for 70% duty cycle case, sawteeth have periods close to τ_{set} because of either partial locking or a coincidental match while decreasing the averaged power. On the other hand, for the 50% case, even with smaller averaged power, τ_{ST} becomes about 140ms; this can be considered as sawtooth locking though phase stability over a longer elapsed time should be demonstrated. On the other hand this result shows that the sawtooth period is controlled by the off-axis ECCD power. This has been used to control series of long sawtooth periods for the study of the effects of sawteeth on impurity transport [23].

In a second experiment, three different modulation periods τ_{set} at fixed duty cycle are used. In the AUG discharge #30552, τ_{set} values are 70, 100 and 140ms (about 0.05, 0.4 and 0.88 in normalised period, respectively) and the duty cycle is constant at 80%. In Fig. 6(a), the experimental traces of the central electron temperature from ECE measurements and the injected EC power are shown. τ_{ST} and τ_{set} are presented in Fig. 6(b) as blue circles and a red line, respectively, and the duty cycle is plotted in the bottom panel. In this experiment, all three EC beams are placed at $\rho_\psi = 0.2$ to test sawtooth *destabilisation* during the first part of the discharge (between 2.0 and 3.0s); subsequently, two EC power sources are turned off while the EC deposition is moved to the stabilising position ($\rho_\psi = 0.42$). At 3.3s, two EC power sources are switched on to stabilise sawteeth. Note that figures 6a-6c show the time from 3.3s onwards, whereas Fig. 6d presents the entire discharge. In the early phase, the sawtooth period is small and irregular, between 10 and 60ms, with an average of 25ms. The interplay with impurity transport/accumulation makes it more difficult to have regular short sawtooth periods. Nevertheless the average sawtooth period during the second phase, 120ms, is clearly much longer than during the destabilization phase.

From 3.3 to 4.1s, continuous EC beams are applied at the fixed position to verify the maximum τ_{ST}. As in the previous case, when EC beams are first switched on, long τ_{ST} occurs during the transient phase and afterwards τ_{ST} decreases to around 125ms. This τ_{ST} is shorter than both that of the previous discharge and the expected sawtooth period from the sweep. From the post-shot analysis, it is shown that the EC deposition position of two beams for sawtooth locking was different from the command: the actual deposition centroids for each launcher are presented in Fig. 6d. They are at slightly different deposition positions from each other and are at $\rho_\psi \sim$0.38 on average, rather than the requested 0.42. From Fig. 4, at this position, τ_{ST} can be between 100 and 140ms, so τ_{ST} of 125ms is not surprising. Note that for the discharge #30550, the beam deposition position was the same as that of the shot #30552: a difference in distances between the deposition position and the $q = 1$ surface may be the reason for the unexpectedly long τ_{ST} in discharge #30550.

From 4.1s the EC beam modulation begins with $\tau_{set} = 70$ms (Fig. 6b - red line) and 80% duty cycle (Fig. 6c). Unfortunately due to a problem of timing, the 70ms phase is much shorter than the other phases; consequently, there is only two sawtooth crashes ($\tau_{ST} \sim 130, 110$ms) and this phase cannot be examined. During the $\tau_{set} = 100$ms phase, there are a few crashes which have τ_{ST} similar to 100ms but overall the sawtooth periods are around 120ms. This suggests that for this plasma equilibrium and average EC deposition location, EC heating during 80ms is sufficient to have essentially the maximum τ_{ST}: 80% is a too high duty cycle, for a 100ms period, to cause the sawtooth cycle to lock to the EC modulation. Indeed from the predictive simulation, it is anticipated that this combination of values is at the edge of the locking region and consequently, will be sensitive to changes in the plasma and launching parameters. For τ_{set} =140ms, the target period is longer than the maximum period possible with continuous injection; therefore, the sawteeth cannot lock to the EC modulation. Near 6.5s, one of EC beams is turned off early and with lower EC power the τ_{ST} decreases after about 0.5s. Note that the transient phase is also about 0.5s when the EC power is turned on, at 3.3s, where the average τ_{ST} is reached only after 3.8s. There are several time scales at play, namely confinement time, current redistribution time, fast particle redistribution and impurity accumulation, which all influence the time evolution of the magnetic shear and thus the sawtooth period.

From Figs. 5 and 6, we tried to determine whether sawteeth lock to the EC pulse or not, based largely on the similarity between τ_{ST} and τ_{set}. To be more clear, the phase of the sawtooth crash relative to the EC modulation period must also be investigated, as shown in Fig. 7. The colours of the

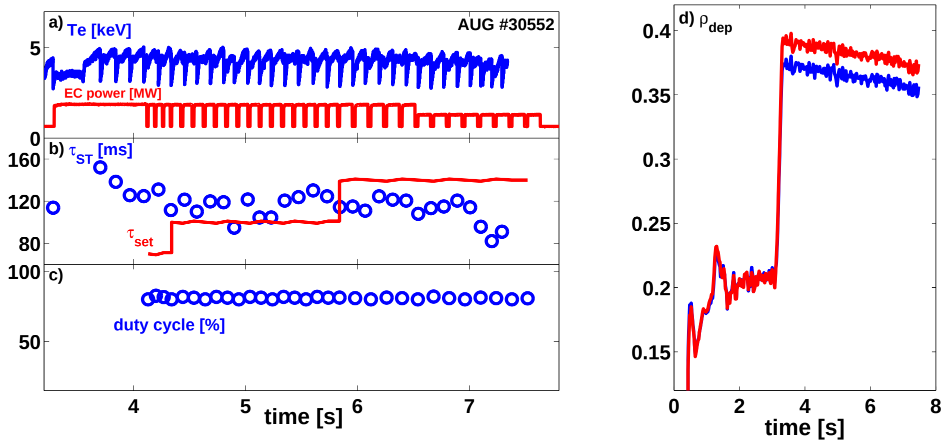

Figure 6: $a) - c)$ EC beams are modulated with τ_{set} of 70, 100 and 140ms and fixed duty cycle of 80%. In all cases, sawteeth do not lock to the EC modulation. $d)$ τ_{ST} is about 125ms with the continuous EC injection at the deposition position $\rho_\psi \sim 0.38$.

vertical bars indicate electron temperature and the length of the bar (y direction) represents τ_{set}: each bar corresponds to one EC modulation cycle. The blue line and black circle denote the EC-on duration and τ_{ST}, respectively. After a crash, the temperature drops quickly to a low value (blue colour) and then recovers more slowly to a higher temperature (red). The alignment of the sudden change to lower temperature indicates that the timing of sawtooth crash is similar to the EC modulation period and that the phase remains constant; one can see if sawteeth are more-or-less locked. For the discharge #30550 (Fig. 7a), we see that with 90% duty cycle τ_{ST} do not match to τ_{set} and the moments of each crash are not regular (i.e. aligned with the modulation): instead, the blue colours form diagonal lines. On the other hand, for the 70% case, sawtooth crashes occur almost right after EC powers are switched off and the blue colours are well aligned horizontally; similar phase alignment is seen at the end of 50% phase, but is not aligned with the turn-off of the EC power. In all phases, the phase alignment is eventually lost (see the end of the 70% phase). At the beginning of 50% phase and the whole phase with 30% duty cycle, sawtooth crashes are never aligned. A similar graphic is presented in Fig. 7b for the discharge #30552. The moment of the crash drifts continually and there is no indication of synchronised sawtoothing. As an example of a successful locking case, the experimental result of TCV discharge #43642 is shown in Fig. 7c. Here, τ_{set} varies between 15, 25 and 35ms with 80% duty cycle. τ_{ST} is well matched to τ_{set} for the 15 and 25ms EC modulation period cases and the drops of temperature are also well aligned and do not drift in time (compare to Fig. 7a near 4 and 6s where, though roughly horizontal, the blue regions still slowly drift downwards and in the long-run locking is lost). For the 15ms case, crashes always occur just after EC power is switched on again, while the crashes always happen just after the EC-off time for 25ms case. For the 35ms, only during the later phase some regulated crashes are observed. In this discharge, regardless of the timing of the sawtooth crash with respect to the EC-off time, the sawtooth instability is considered to be locked only when it is well regulated for 10 or more cycles by the EC pulse. Note that after an initial transition phase (a few cycles), the jitter in crash timing becomes small and apparently random.

In the two AUG discharges, the maximum τ_{ST} for a fixed aiming turned out to be different from the expected one, so one cannot compare them in absolute terms. For this reason, we have put the experimental cases on the normalised locking range with the simulation results in Fig. 2 (shown in Sec. 2.1). Since the experimental condition was different from the predictive simulation (#30233) and we did not have a full scan of a locking range from the experiments, we carried out the same simulations with experimental data. Since we have seen that #30550 and #30552 have different plasma states, the experimental data from #30543 was taken to estimate a locking range. Based on the simulation result from AUG #30543, the experimental results from two locking discharges are presented. The simulation results aiming for the maximum sawtooth period of 145ms are represented by blue circles (locking), red crosses (non-locking) and blue crosses (twice or three times of the chosen τ_{set}). The green squares show the predicted simulation results using AUG #30233 data which are quite similar despite the different plasma conditions and auxiliary heating powers. The AUG #30550 discharge cases are indicated by stars.

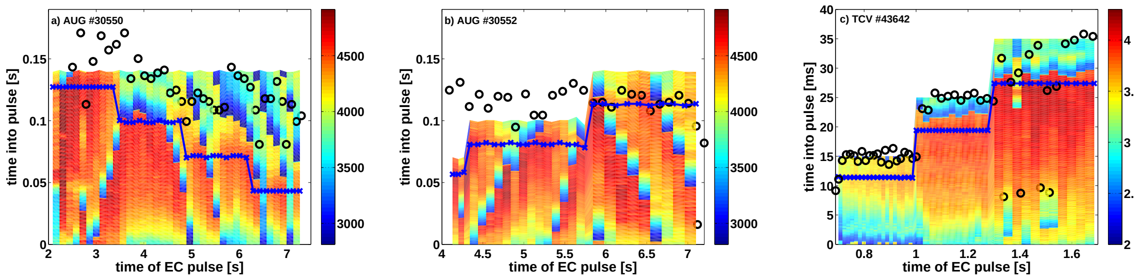

Figure 7: The change of temperature during modulation periods are shown with τ_{ST} and EC pulse on time for (a) AUG #30550, (b) AUG #30552 and (c) TCV #43642. The vertical colour bars indicate electron temperature at plasma centre and the black circle and blue line represent sawtooth period and EC-on duration, respectively. When sawteeth lock to EC modulation, the change of temperature aligns well while the timing is random or drifts for non-locking case.

Since the exact value of the maximum and reference periods for the discharge #30550 are unknown, the upper and lower boundary of the *expected* normalised periods for this case are marked as black dashed lines. The 30% duty cycle case is located outside the successful locking range, locking is expected for the 50 and 70% cases, and the 90% case may lie just outside the locking range. These are somewhat similar to, but not precisely the same as, the experimental result; in particular, the 50 and 70% cases do not really lock. However it is only during these two phases, 50 and 70% duty cycle, that we find 4 consecutive sawteeth with τ_{ST} near target with a very different average power per cycle (near 4s and 6s in Fig. 5). We also see in Fig. 2 that these cases are near the border of the locking region, hence simulation and experimental results are consistent in this respect. The triangles in Fig. 2 denote the results from AUG #30552. For the 70ms modulation period, the 80% duty cycle case is far from the successful locking range ($\tau_{normalised} \approx 0.1$) and for the 100ms period, it is close to the edge of the locking region (as in the #30550 90% case). Since the deposition positions relative to the $q = 1$ surface were different for each discharge, the expected locking range may differ accordingly as discussed in Refs. [10, 19]. In particular, for the discharge #30552, because the heating position relative to the $q = 1$ surface is further towards the axis, a narrower successful locking range is anticipated. This is a possible explanation for unsuccessful locking. Based on this analysis, additional simulations and experiments should be performed to explore the possible locking ranges in different positions, to demonstrate clear locking, and to better understand the present results. Compared to recent sawtooth locking experiments on TCV [11] and KSTAR [12] plasmas, AUG plasmas appear to require more time to adjust to the EC modulation; the transition period is longer. Hence, for a clear demonstration, experiments using a more simple set-up may need to be performed with one τ_{set} and one duty cycle during a whole discharge, near 50-60% duty cycle and $\tau_{normalised} \approx 0.5$ as seen in Fig. 2. This should allow an investigation of the transition dynamics to locking itself and allow better prediction capability for further experiments. Furthermore, it would be helpful to map the full locking range, to be compared to the simulation results, but this would require a significantly larger number of discharges, which is out of the scope of present experimental constraints. Nevertheless it would help improve the simulations know-how as well. In particular the impurity accumulation, which influence the effective T_e profile in the center, and the fast particle redistribution due to sawteeth, which influence the effective IC deposition, are not included in the present model.

In order to investigate the behaviour of sawtooth on different tokamaks, the experimental results are compared to TCV and KSTAR sawtooth locking experiments and ITER predictive simulations. Since the main focus of sawtooth control is to regulate the moment of the sawtooth crash and to predict the timing of a consequent island formation, we compared the time delays of the sawtooth crash after EC power is turned off since this indicates the time available on which to actuate pre-emptive ECCD on the expected NTM location. Similar to sawtooth pacing, successful locking cases mostly have sawtooth crashes during EC off phase, thus the time delay can be defined as the time difference between the crash and EC power off ($t_{crash} - t_{ECoff}$). The estimated time delays from AUG, KSTAR and TCV experiments and ITER simulation results are shown in Fig. 8. For AUG (blue circles), several crashes that occur during the EC off phase are taken from #30550. Similar cases from KSTAR (#9146, red crosses) [12] and TCV (#43641, 42, 45, 47, 85, 86, green squares) [11] locking experiments are selected to compare to AUG results. For the ITER case [19] (violet diamonds), sawtooth pacing simulation results with different power levels and heating positions are taken for comparison. All the time delays are normalised by their sawtooth periods and $\tau_{set}^{normalised}$, defined in the same way as the one described earlier, is used for the abscissa. Note that in this figure τ_{set} is defined in the same way as for sawtooth pacing; the time difference between EC power off and preceding sawtooth crash. As seen in Fig. 8, despite the different conditions such as machine specifications, plasma current, energy confinement time and auxiliary heating system (TCV: ECH/CD, KSTAR: ECH/CD, NBI, AUG & ITER: ECH/CD, NBI, ICH), all the normalised delays show similar curves as a function of normalised modulation periods. Although the experimental and simulation data sets are limited, they provide a reasonable starting point for elaborating a scaling law for the time delay to the sawtooth crash. It is expected that using the scaling law, sawtooth crashes can be regulated by EC modulation and the resultant NTM triggering can be mitigated.

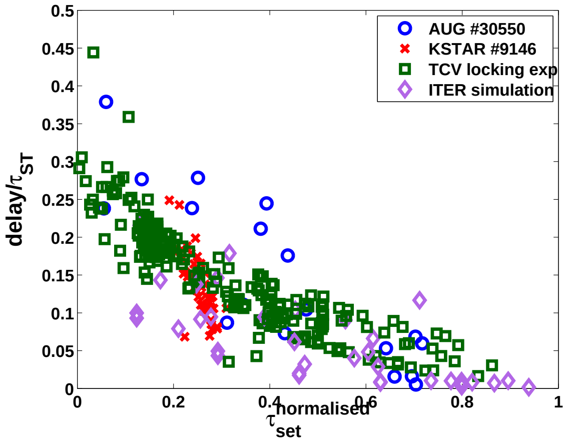

Figure 8: The time delays between sawtooth crashes and the EC power off from AUG, KSTAR, TCV and ITER (simulations) show a similar tendency despite of different machine sizes and operational conditions.

4 Conclusion

In this study, we have extended sawtooth control using EC power modulation, demonstrated on the TCV and KSTAR tokamaks, to AUG plasmas using the sawtooth locking method in the presence of fast particles produced by NBI and IC auxiliary heating and impurity peaking control. From predictive simulation performed prior to the main experiment, the possible locking range was determined. Based on the simulations and sweeping experiment, sawtooth locking experiments were carried out with various EC modulation periods and duty cycles. From a scan of the EC deposition location across the $q = 1$ radius, a target $\rho_\psi = 0.42$ yielding a sawtooth period of 150ms with continuous EC power injection was anticipated and 90 to 30% duty cycles and 100 and 140ms with 80% duty cycle were chosen. The following experimental discharges with varying duty cycle and modulation frequency turned out to have slightly different effective plasma parameters. In this way the CW stabilised sawtooth period was different as well as the effective deposition location with respect to the $q = 1$ radius (a small but significant difference). Nevertheless, control of the sawtooth period with co-ECCD was clearly demonstrated, leading to reliable series of long sawtooth periods, in the presence of fast particles from NBI and IC powers and of impurity accumulation control (with central EC). These experiments can be extended to ITER for sawtooth period control with all the possible heating systems in the presence of α-particles. On the other hand, proper locking was not obtained. Small series of sawtooth periods close to the target modulation frequency have been obtained with 50% and 70% duty cycles, however detailed analysis of the phase between the sawtooth crashes and the EC power show a slow drift with time.

The present experimental scenarios are combining the complexities of the time evolution of the electron temperature and q profiles, the main driver of the time evolution of the magnetic shear at the $q = 1$ surface, with the role of impurity accumulation and of the redistribution of the fast particles at crashes after long sawtooth periods which influence the time evolution of T_e and the IC deposition location, respectively. The maximum sawtooth period obtained with CW co-ECCD, with pre-determined launcher angles, was therefore not constant from shot to shot. Nevertheless, guided by the simulations results, one can normalise the modulation and sawtooth periods. In this way, we have shown that the experimental and the simulation results are consistent but not fully identical. In particular it shows that the experimental cases turned out to be at the edge of the predicted locking range. To confirm this result and the possibility to obtain full locking in such scenarios, new experiment need to be carried out with a duty cycle of 50-60% and a normalised target sawtooth period of 0.5-0.6 (see Fig. 2). These results will also demonstrate the role of fast particles redistribution and impurity accumulation, and help in including these effects in the simulation model.

The AUG experiment has again demonstrated what was previously found on other tokamaks; that the distance between the EC deposition and the $q = 1$ surface is an important parameter. Recently, real-time equilibrium reconstruction codes such as the real-time version of LIUQE: RT-LIUQE [24] have been used to estimate the q profile in real-time. Initial experiments indicate that due to various data errors and offsets, the exact position of the $q = 1$ surface cannot be accurately determined - this is inherent in the fact that the shear near the plasma centre is relatively small, so small errors in q result in large errors in ρ_ψ. Thus, at present, the EC deposition cannot track accurately the $q = 1$ surface and as a result the effect of EC injection varies strongly with the details of the plasma equilibrium. Real-time transport codes such as RAPTOR [25] may be a tool to better estimate the correct position once the effects of the EC waves on the current profile is included in the equilibrium reconstruction. This kind of code can evaluate transport equations combining the experimental data and the equilibrium calculation. Therefore it is expected that sawtooth control will be continually improved in future experiments.

The time delays between sawtooth crashes and EC power off times were compared to those from TCV and KSTAR sawtooth locking experiment and ITER predictive pacing simulation results. All the tokamaks that were studied have different sizes, machine characteristics, energy confinement time scales and sawtooth periods. In addition, the auxiliary heating systems are different. Despite those differences, the normalised time delays showed a similar dependence on the normalised set (or "on") time - with a decreasing normalised delay for an increasing normalised τ_{set}. This provides further evidence that the predicted simulations provide relevant information. It also shows that sawtooth pacing should allow an easier control of AUG sawtooth periods. Indeed the delay is relatively long on AUG, which can lead to sawtooth period slightly longer than expected and a sawtooth crash occuring after the turn-on of the EC power, when the EC modulation period is set before-hand. On the other hand, with pacing and real-time detection of the sawtooth crash, the EC power waveform can be adapted in real-time to the last sawtooth period, yielding a more accurate and reliable control of the effective sawtooth period. A real-time sawtooth detector has been recently developed for AUG [26] and therefore AUG can now compare pacing and locking experiments in the complex scenarios including fast particles from NBI and ICRH, impurity accumulation control and co-ECCD.

These experiments demonstrate the risks associated with performing complex experiments in tokamaks using a minimum number of discharges to elucidate a maximum amount of physics - even when based on a solid support from simulation and experimental results from other tokamaks. Though a demonstration of sawtooth locking was sought, it was hoped that an investigation of the locking map could also be accomplished. The results presented here show that new physics (impurity accumulation, fast ion redistribution) need be investigated in a dedicated way to improve the ability of simulations to predict future experiments in tokamaks with metal walls and IC heating.

Acknowledgements

D. Kim would like to thank Dr. E. Fable for providing reference data for ASTRA simulation. This work has been carried out within the framework of the EUROfusion Consortium and has received funding from the Euratom research and training programme 2014-2018 under grant agreement No 633053. This work was supported in part by the Swiss National Science Foundation and by the Principality of Monaco/ITER Postdoctoral Research Fellowship Program. The views and opinions expressed herein do not necessarily reflect those of the European Commission and ITER Organization.

References

[1] F. Porcelli, D. Boucher, and M.N. Rosenbluth. "Model for the sawtooth period and amplitude". *Plasma Phys. Control. Fusion*, 38(12):2163, 1996.

[2] G.P. Canal et al. "Fast seeding of NTMs by sawtooth crashes in TCV and their preemption using ECRH". *Nucl. Fusion*, 53(11):113026, 2013.

[3] I.T. Chapman et al. "Power requirements for electron cyclotron current drive and ion cyclotron resonance heating for sawtooth control in ITER". *Nucl. Fusion*, 53(6):066001, 2013.

[4] O. Sauter et al. "Control of Neoclassical Tearing Modes by Sawtooth Control". *Phys. Rev. Lett.*, 88(10), 2002.

[5] F. Felici et al. "Integrated real-time control of MHD instabilities using multi-beam ECRH/ECCD systems on TCV". *Nucl. Fusion*, 52(7):074001, 2012.

[6] T.C. Hender et al. "Chapter 3: MHD stability, operational limits and disruptions". *Nucl. Fusion*, 47(6):S128, 2007.

[7] O. Sauter et al. "On the requirements to control neoclassical tearing modes in burning plasmas". *Plasma Phys. Control. Fusion*, 52(2):025002, 2010.

[8] I.T. Chapman et al. "Empirical scaling of sawtooth period for onset of neoclassical tearing modes". *Nucl. Fusion*, 50(10):102001, 2010.

[9] T.P. Goodman et al. "Sawtooth pacing by real-time auxiliary power control in a tokamak plasma". *Phys. Rev. Lett.*, 106(24), 2011.

[10] G. Witvoet et al. "Numerical demonstration of injection locking of the sawtooth period by means of modulated EC current drive". *Nucl. Fusion*, 51(10):103043, 2011.

[11] M. Lauret et al. "Demonstration of sawtooth period locking with power modulation in TCV plasmas". *Nucl. Fusion*, 52(6):062002, 2012.

[12] J.H. Jeong et al. "Demonstration of sawtooth period control with EC waves in KSTAR plasma". *EPJ Web of Conferences*, 87:02016, 2015.

[13] G.V. Pereverzev and P.N. Yushmanov. *"ASTRA Automated System for Transport Analysis"*. Max-Planck-Institut für Plasmaphysik, Rep. IPP 5/98, Garching, February 2002.

[14] D. Kim et al. "Simple predictive electron transport models applied to sawtoothing plasmas". *Plasma Phys. Control. Fusion*, 58(5):055002, 2016.

[15] C. Angioni and O. Sauter. "Neoclassical transport coefficients for general axisymmetric equilibria in the banana regime". *Phys. Plasmas*, 7(4):1224, 2000.

[16] B. Kadomtsev. "On disruptive instability in tokamaks". *Soviet Journal of Plasma Physics*, 1(5):710, 1975.

[17] O. Sauter et al. "Sawtooth period simulations of TCV discharges". In *Proc. Joint Varenna-Lausanne Int. Workshop on Theory of Fusion Plasmas, Varenna, Italy, August, 1999*, 1998.

[18] C. Angioni et al. "Neoclassical transport coefficients for general axisymmetric equilibria in the banana regime". *Nucl. Fusion*, 43(6):455, 2003.

[19] D. Kim, T.P. Goodman, and O. Sauter. "Real-time sawtooth control and neoclassical tearing mode preemption in ITER". *Phys. Plasmas*, 21(6):061503, 2014.

[20] E. Poli, A.G. Peeters, and G.V. Pereverzev. "TORBEAM, a beam tracing code for electron cyclotron waves in tokamak plasmas". *Comput. Phys. Commun.*, 136(1-2):90, 2001.

[21] A. Mück et al. "Sawtooth control experiments on ASDEX Upgrade". *Plasma Phys. Control. Fusion*, 47(10):1633, 2005.

[22] M. Maraschek et al. "Active control of MHD instabilities by ECCD in ASDEX Upgrade". *Nucl. Fusion*, 45(11):1369, 2005.

[23] M. Sertoli et al. "Interplay between central ECRH and MHD in mitigating tungsten accumulation in ASDEX Upgrade". In *Proceedings of the 42nd EPS conference*, volume 39E, pages O4.129, ISBN 2–914771–98–3, Lisbon, Portugal, 2226 June, 2015.

[24] J.M. Moret et al. “Tokamak equilibrium reconstruction code LIUQE and its real time implementation”. *Fusion Eng. Des.*, 91(2):1, 2015.

[25] F. Felici et al. “Real-time physics-model-based simulation of the current density profile in tokamak plasmas”. *Nucl. Fusion*, 51(8):083052, 2011.

[26] H. Van den Brand et al. “A model-based, multichannel, real-time capable sawtooth crash detector”. *Plasma Phys. Control. Fusion*, 58(7):075002, 2016.